

Optical Spectroscopic Studies on Penning Ionization and Charge-Transfer Reactions at Thermal Energy by Using Flowing Afterglow

Tsuji, Masaharu
Institute of Advanced Material Study Kyushu University

Nishimura, Yukio
Institute of Advanced Material Study Kyushu University

<https://doi.org/10.15017/6583>

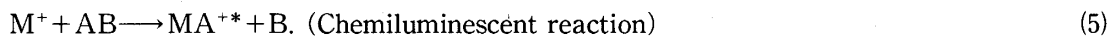
出版情報 : 九州大学機能物質科学研究所報告. 4 (2), pp.163-174, 1991-03-30. 九州大学機能物質科学
研究所
バージョン :
権利関係 :

Optical Spectroscopic Studies on Penning Ionization and Charge-Transfer Reactions at Thermal Energy by Using Flowing Afterglow

Masaharu TSUJI and Yukio NISHIMURA

The flowing afterglow apparatus has been coupled with a low pressure chamber by a small orifice for optical spectroscopic studies on Penning ionization and charge-transfer reactions under single collision conditions. Nascent rovibrational distributions are determined from a spectral simulation. As selected examples, detailed results are reported about non-Franck-Condon type $\text{He}(2^3\text{S})/\text{O}_2$ Penning ionization and near-resonant $\text{He}^+/\text{H}_2\text{O}$, D_2O charge-transfer reactions. A brief summary is also given of our optical spectroscopic studies by using the conventional flowing afterglow apparatus.

The flowing afterglow (FA) method was developed in 1963 by Ferguson and his co-workers of NOAA Laboratories in Boulder, Colorado, for the study of ion-molecule reactions in the earth's atmosphere.¹⁾ The main emphasis of their studies was placed upon measurements of formation rate constants and branching ratios of ionic products by using a mass spectrometer. More than a few thousands kinetic data at (near) thermal energy were compiled in the reported tables.²⁾ In our laboratory, the FA coupled with a UV and visible emission detection system has been used for studying the following ionization processes in collisions of metastable atoms (M^*) and ions (M^+) with a molecule (AB):



One purpose of our FA optical study is the detection of new ion fluorescences, which are difficult to excite by photoionization and electron-impact ionization. In Table 1 are listed ion fluorescences identified in our laboratory and their ionization processes. During spectroscopic studies on new fluorescences of group IV monohalide ions, broad visible bands have been found in reactions of He^* and/or Ne^* with SiCl_4 ,^{6, 7)} GeCl_4 ,⁸⁾ and SiBr_4 .⁹⁾ Although these emissions have been ascribed to neutral XY_2^* and/or XY_2^+ fragments, they are reassigned to the $\tilde{\text{C}}^2\text{T}_2 - \tilde{\text{A}}^2\text{T}_2$ and $\tilde{\text{C}}^2\text{T}_2 - \tilde{\text{X}}^2\text{T}_1$ bound-free transitions of parent cations (XY_2^{+*}).¹⁰⁾ A recent optical study on SiBr_2^+ by electron-

Optical Spectroscopic Studies on Ionization Processes by Using Flowing Afterglow

 Table 1 Ionic emissions identified in Kyushu University.³⁻⁵⁾

Ions	Transitions	Reactions
CS ⁺	B ² Σ ⁺ - A ² Π	He ⁺ /CS ₂ , OCS
	B ² Σ ⁺ - X ² Σ ⁺	He*, Ne*/CS
PN ⁺	B ² Σ ⁺ - X ² Σ ⁺	He*, Ne*/PN
SO ⁺	A ² Π - X ² Π _r	He ⁺ /SO ₂
S ₂ ⁺	A ² Π - X ² Π _r	He ⁺ /S ₂ Cl ₂
CCl ⁺	A ¹ Π - X ¹ Σ ⁺	He ⁺ /CCl ₄
	a ³ Π ₁ - X ¹ Σ ⁺	He ⁺ /CCl ₄
SiCl ⁺	a ³ Π _{0,1} - X ¹ Σ ⁺	He ⁺ /SiCl ₄
GeCl ⁺	a ³ Σ ⁺ - X ¹ Σ ⁺	He ⁺ /GeCl ₄
SnCl ⁺	a ³ Σ ⁺ - X ¹ Σ ⁺	He ⁺ /SnCl ₄
CBr ⁺	A ¹ Π - X ¹ Σ ⁺	He ⁺ /CBr ₄
	a ³ Π _{0,1} - X ¹ Σ ⁺	He ⁺ /CBr ₄
SiBr ⁺	a ³ Π _{0,1} - X ¹ Σ ⁺	He ⁺ /SiBr ₄
BBr ⁺	A ² Π - X ² Σ ⁺	He ⁺ /BBr ₄
GeH ⁺	a ³ Π _{0,1} - X ¹ Σ ⁺	He*, He ⁺ /GeH ₄
SnH ⁺	a ³ Π _{0,1} - X ¹ Σ ⁺	He*, He ⁺ /SnH ₄

 Table 2 Ionization processes studied by using conventional FA apparatus^{3, 12-18)}

Reactants	Targets	Product ions
Pennig Ionization		
He*	N ₂	N ₂ ⁺ (B ² Σ ⁺)
He*	CO	CO ⁺ (A ² Π, B ² Σ ⁺)
He*, Ne*	HCl, HBr	HCl ⁺ , HBr ⁺ (A ² Σ ⁺)
He*, Ne*	CS	CS ⁺ (B ² Σ ⁺)
He*, Ne*	PN	PN ⁺ (B ² Σ ⁺)
He*	CO ₂	CO ₂ ⁺ (A ² Π, B ² Σ ⁺)
He*, Ne*	N ₂ O	N ₂ O ⁺ (A ² Π)
He*, Ne*	OCS	OCS ⁺ (A ² Π)
He*, Ne*	CS ₂	CS ₂ ⁺ (A ² Π)
He*, Ne*	ICN	ICN ⁺ (A ² Σ ⁺)
He*	H ₂ S	SH ⁺ (A ³ Π)
He*, Ne*, Ar*	X-(C≡C) ₂ -X (X=H, CH ₃ , C ₂ H ₅)	X-(C≡C) ₂ -X ⁺ (A ² Π)
Charge-transfer reaction		
He ⁺	N ₂ O	N ₂ O ⁺ (A ² Σ ⁺) N ₂ ⁺ (B ² Σ ⁺)
He ⁺	CO ₂	CO ⁺ (A ² Π)
He ⁺ , Ne ⁺	OCS	CO ⁺ (A ² Π)
He ⁺	SiBr ₄	SiBr ⁺ (a ³ Π _{0,1})
He ⁺	GeCl ₄ , SnCl ₄	GeCl ₄ ⁺ , SnCl ₄ ⁺ (a ³ Σ ⁺)
He ₂ ⁺	CO ₂	CO ₂ ⁺ (A ² Π, B ² Σ ⁺)
He ₂ ⁺	S ₂ Cl ₂	S ₂ ⁺ (A ² Π)
Ar ⁺ , N ₂ ⁺	OCS	OCS ⁺ (A ² Π)
He ₂ ⁺ , Ne ₂ ⁺	N ₂	N ₂ ⁺ (B ² Σ ⁺)
He ₂ ⁺	CO	CO ⁺ (A ² Π, B ² Σ ⁺)
Ar ⁺	HCl, DBr	HBr ⁺ , DBr ⁺ (A ² Σ ⁺)
Ar ⁺	CS	CS ⁺ (B ² Σ ⁺)
Ar ⁺	PN	PN ⁺ (B ² Σ ⁺)
Ar ₂ ⁺	H-(C≡C) ₂ -H	H-(C≡C) ₂ -H ⁺ (A ² Π)
Ar ₂ ⁺ , CO ⁺	CS ₂	CS ₂ ⁺ (A ² Π)
Chemiluminescent reaction		
C ⁺	O ₂ , CO ₂ , NO ₂ , N ₂ O	CO ⁺ (A ² Π)
C ⁺	N ₂ O	CN(A ² Π)
C ⁺	CS ₂ , OCS	CS ⁺ (A ² Π)

impact supports this assignment.¹¹⁾

The other purpose is the analysis of internal state distribution for an understanding of ionization dynamics at the microscopic level. Ionization processes studied by our group are summarized in Table 2. Until our FA optical research, the FA coupled with UV and visible emission spectroscopy has dominantly been used for product state analysis in energy transfer reactions by metastable species such as $\text{Ar}(^3\text{P}_{0,2})$, $\text{He}(2^3\text{S})$, and $\text{N}_2(\text{A}^3\Sigma_u^+)$. In most cases, ionic active species involved in the discharge flow has been treated as impurities. Combining a microwave discharge source with a high-capacity pumping system (10,000 ℓ/min), the FA optical studies were extended to various types of ion-molecule reactions. The overlap of emissions due to ionic reactions with those due to metastable reactions has often made detailed FA optical studies on ion-molecule reactions difficult. This problem has been overcome by using a pulse modulation technique, where emissions from ionic reactions can be detected exclusively.¹⁹⁾

Advantages of the FA optical method are as follows.

(1) Because of a high ion density, emission intensity is strong. Therefore, the detection limit of an emission system is low ($\sim 10^{-15} \text{ cm}^3\text{s}^{-1}$), and high resolution measurements that can separate rovibrational structures effectively are possible in most cases.

(2) Product state analysis in ion-molecule reactions is possible at thermal energy, where the application of beam experiments is difficult.

A great disadvantage of the FA method is that initial internal state distributions are often modified or lost by collisions with buffer gas, because operating pressures are rather high. This effect is especially severe for molecules with long radiative lifetimes ($> 1\mu\text{s}$) and large quenching rate constants. In order to overcome this problem, the FA apparatus has recently been combined with a

Table 3 Ionization processes studied by using the FA apparatus coupled with a low pressure chamber

Reactants	Targets	Product ions	Refs.
Penning ionization			
He^*	O_2	$\text{O}_2^+(\text{A}^2\Pi_u)$	20
He^*	CO	$\text{CO}^+(\text{A}^2\Pi)$	21
He^*	HCl, HBr	$\text{HCl}^+, \text{HBr}^+(\text{A}^2\Sigma^+)$	22
He^*	CS_2	$\text{CS}_2^+(\text{A}^2\Pi)$	23
Charge-transfer reaction			
He^+	N_2	$\text{N}_2^+(\text{D}^2\Pi)$	24
He^+	$\text{H}_2\text{O}, \text{D}_2\text{O}$	$\text{OH}^+, \text{OD}^+(\text{A}^3\Pi)$	25
He^+	C_2H_2	$\text{CH}^+(\text{A}^1\Pi)$	26
He^+	SiH_4	$\text{SiH}^+(\text{A}^1\Pi)$	27
He^+	CS_2	$\text{CS}^+(\text{B}^2\Sigma^+)$	
He^+	OCS	$\text{CO}^+(\text{A}^2\Pi)$	
He^+	CO	$\text{CO}^+(\text{A}^2\Pi, \text{B}^2\Sigma^+)$	
Ar^+	H_2O	$\text{H}_2\text{O}^+(\text{A}^2\text{A}_1)$	

low pressure cell by a small orifice. This beam apparatus was successfully applied to studying Penning ionization and charge-transfer reactions. Ionization processes that have been investigated by our group are listed in Table 3. Among our studies, He(2^3S)/O₂ Penning ionization and He⁺/H₂O, D₂O charge-transfer reactions are presented in this review as selected examples.

EXPERIMENTAL

The beam apparatus used in this study is shown in Fig. 1. It is composed of two parts, a source chamber and a reaction cell. Rare gas active species were generated by a microwave discharge in the source chamber operated at 0.05-1.0 Torr (1 Torr = 133 Pa). After thermalized in the discharge flow, they were expanded into a low-pressure collision chamber through a 2.0 mm diam orifice. The contribution of ionic active species to the observed emissions was examined by using an ion-collector grid placed in front of the orifice. Target gases were introduced through a stainless steel nozzle located about 3 mm downstream from the orifice. The partial pressure in the collision chamber was 0.5-1 mTorr for rare gas and 0.5-2 mTorr for target gases. The emission spectrum was dispersed by a 1.0 m scanning monochromator equipped with a cooled photomultiplier.

RESULTS AND DISCUSSION

He(2^3S)/O₂ Penning ionization. Penning ionization of O₂ by metastable He(2^3S) atoms leading to O₂⁺(A²Π_u) has captured the attention since Robertson²⁸⁾ and Richardson *et al.*^{29, 30)} found non-Franck-Condon (FC) vibrational distribution of O₂⁺(A²Π_u) in their FA studies using optical spectroscopy (PIOS):



Penning ionization (6) consists of the following steps:

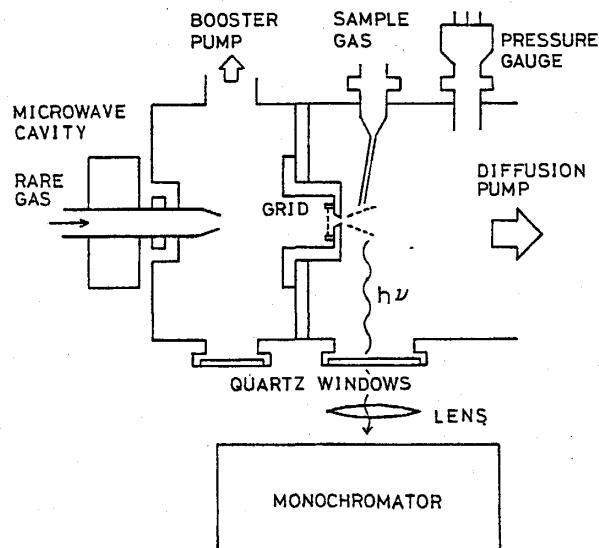


Fig. 1 The flowing afterglow apparatus coupled with a low pressure chamber.



Penning ionization electron spectroscopy (PIES) method has also been used to the study of $\text{He}(2^3\text{S}, 2^1\text{S})-\text{O}_2$ Penning ionization.³¹⁻³⁴⁾ Since the PIES method measures a kinetic energy distribution of Penning electrons ejected in process (8), a comparison of the PIES data and FC factors for ionization provides information on an interaction in the entrance channel. On the other hand, the PIOS method detects photoemission from excited ions in process (10), and then gives information on an interaction in the exit channel by comparison with the PIES data. Although a weak PIES peak of $\text{O}_2^+(A)$ was identified,³¹⁻³⁴⁾ it was very broad and heavily overlapped with the $a^4\Pi_u$ and $b^4\Sigma_g^-$ bands. Therefore, the vibrational distribution and the peak shift have not been determined. In the present PIOS study, the nascent rovibrational distribution of $\text{O}_2^+(A)$ has been determined by observing the $\text{O}_2^+(A-X)$ emission in the beam experiment.

In Figs. 2a) and 2c) are compared emission spectra obtained from the $\text{He}(2^3\text{S})/\text{O}_2$ reaction in the beam and FA experiments. The $\text{O}_2^+(A-X)$ emission system from $v'=0-13$ and weak atomic oxygen lines are identified in both spectra. The maximum intensity of the beam spectrum shifts to blue and the fraction of the underlying continuum is large in comparison with the FA spectrum due to higher vibrational and rotational excitation. The rovibrational distribution in $\text{O}_2^+(A : v'=0-13)$ was determined by a computer simulation of the observed spectra, because a number of vibronic transitions are heavily overlapped. In Figs. 2c) and 2d) are shown the best fit FA and beam spectra, respectively, obtained assuming a single Boltzmann rotational distribution for each v' level. The rovibrational distributions thus obtained are given in Table 4 together with reported FA data of Richardson and Setser³⁰⁾ and RKR FC factors for $\text{O}_2(X) \rightarrow \text{O}_2^+(A)$ vertical ionization.

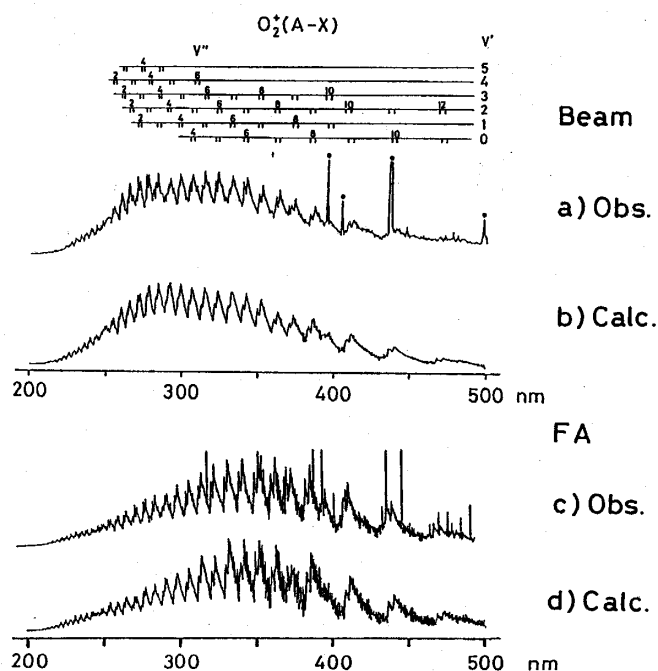


Fig. 2 Observed and calculated $\text{O}_2^+(A-X)$ emissions produced from the $\text{He}(2^3\text{S})/\text{O}_2$ Penning ionization in the beam and flowing afterglow experiments.

Optical Spectroscopic Studies on Ionization Processes by Using Flowing Afterglow

 Table 4 Rovibrational distributions of $O_2^+(A^2\Pi_u)$ produced from the $He(2^3S)-O_2$ Penning ionization.^{a)}

		$v'=0$	1	2	3	4	5	6	7	8	9	10	11	12	13
Beam ^{b)}	$N_{v'}$	100	83	54	35	26	19	10	7.4	4.6	2.9	1.9	0.93	0.74	0.46
	$T_R(K)$	4200	3500	2800	2200	1700	1400	1000	800	600	600	600	400	400	400
FA ^{c)}	$N_{v'}$	100	61	21	7.4	6.8	5.0	3.9	2.6	2.2	1.5	1.0	0.78	0.43	0.26
	$T_R(K)$	3100	2400	2000	1600	1300	1100	800	600	500	400	400	400	300	300
FA ^{d)}	$N_{v'}$	100	94	63	47	22	22	—	—	—	—	—	—	—	—
FCF ($\times 10^{-3}$) ^{e)}		2.8	12	29	49	68	82	89	89	84	76	67	57	48	40
		(3.1)	(14)	(32)	(55)	(77)	(92)	(100)	(100)	(95)	(86)	(75)	(64)	(54)	(45)

a) Uncertainties of the present data are $\pm 7\%$.

b) This work.

c) This work: flowing afterglow at a He pressure of 0.37 Torr.

d) Ref. 30: flowing afterglow at a He pressure of 2.0 Torr.

e) Franck-Condon factors calculated by using RKR potentials. Relative values are given in parentheses.

A comparison of our beam and FA data implies that the $O_2^+(A)$ ions are relaxed both vibrationally and rotationally in the FA conditions by collisions with the buffer He gas. It should be noted that the FA result of Richardson and Setser at a He pressure of 2 Torr³⁰⁾ is more vibrationally excited than our FA result at 0.37 Torr and the beam one at 1 mTorr. The $O_2^+(A-X)$ emission resulting from the He_2^+/O_2 reaction in the He afterglow was much more vibrationally excited than that from the $He(2^3S)/O_2$ reaction.²⁰⁾ Therefore, the most probable explanation of the high vibrational excitation in their FA data is the contribution of the He_2^+/O_2 charge-transfer reaction because

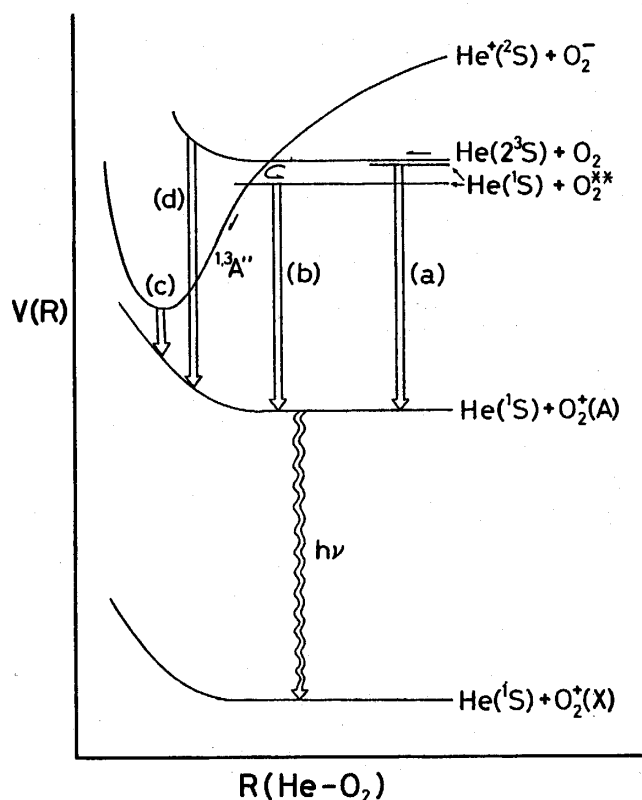


Fig. 3 Potential energy curves for the $He(2^3S)/O_2$ Penning ionization leading to $O_2^+(A^2\Pi_u)$ ions. O_2^{**} denotes Rydberg states.

of incomplete ion collection.

The nascent vibrational distribution has a peak at $v'=0$ and decreases rapidly with increasing v' . This differs markedly from FC factors for vertical ionization with a peak around $v'=7$. The rotational temperature decreases rapidly from 4200 K for $v'=0$ to 400 K for $v'=13$. The present PIOS data represent that 295 meV and 257 meV are deposited into vibration and rotation of $O_2^+(A)$ in process (6), respectively. This shows that 10.6% and 9.3% of the total available energy are partitioned into vibration and rotation, respectively.

The following four cases are possible to explain the non-FC like vibrational population of $O_2^+(A)$; each case is shown in Fig. 3.

Case (a): (near) resonant excitation transfer: this process proceeds through excitation transfer from the covalent $^1,^3A''$ He(2^3S)– O_2 entrance potentials to a (near) resonant Rydberg potential followed by autoionization into the exit ionic potential.

Case (b): pseudo-resonance excitation transfer via an ionic potential; this process proceeds through an avoided crossing from the covalent entrance potential to the $He^+ - O_2^-$ ionic potential followed by a second avoided crossing onto an O_2^{*} Rydberg potential, from which autoionization takes place.

Case (c): ionization via an ionic potential; this process results from an avoided crossing from the He(2^3S)– O_2 covalent potentials to the $He^+ - O_2^-$ ionic potentials followed by a direct autoionization into the product He– $O_2^+(A)$ potential.

Case (d): Penning ionization from an entrance covalent surface; a transition from the covalent into ionic configuration is symmetrically forbidden in $C_{\infty v}$ and C_{2v} symmetries for the He($1s2s$)– O_2 quasi-molecule system.³⁴⁾ Hence, the He(2^3S)– O_2 quasi-molecule system survives the crossing in the covalent conformation, if the symmetries is either $C_{\infty v}$ or C_{2v} when the crossing radius is reached.

In cases (a) and (b) Penning ionization occurs at rather long range where the exit surface is nearly flat, while it does at short range in cases (c) and (d) where the exit surface is repulsive. The latter processes probably play a significant role for the formation of $O_2^+(A)$ because the high rotational excitation is likely to result from a short-range repulsive interaction in the exit [He– $O_2^+(A)$ →He+ $O_2^+(A)$] channel. A strong underlying continuum probably due to a strongly attractive entrance potential is present in the PIES spectrum.^{31–34)} An additional evidence of the presence of an attractive entrance surface in process (7) has recently been obtained by the dependence of partial ionization cross section of $O_2^+(A)$ on the reactant energy in a PIES study of Mitsuke *et al.*³⁵⁾ On the basis of these facts, it is reasonable to assume that the dominant ionization occurs via case (c) and a significant $V \rightarrow T, R$ transfer in the exit channel is the major determinant of the observed non-FC like vibrational distribution accompanied by high rotational excitation for low v' levels.

He⁺/H₂O, D₂O dissociative charge-transfer. Figs. 4a) and 4c) show emission spectra produced from the He⁺, He(2^3S)/H₂O reactions in the beam and FA experiments, respectively. The

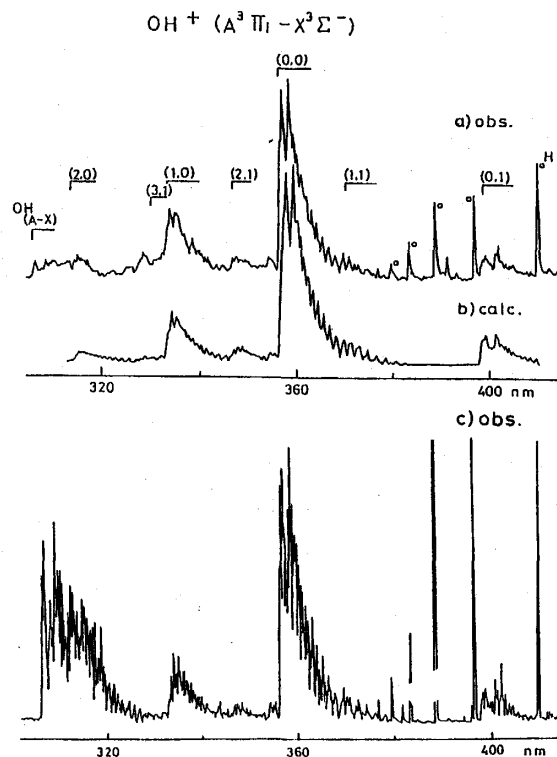


Fig. 4 Emission spectra of H_2O .
(a) Beam: obs. (b) Beam: Calc. (c) FA: Obs.

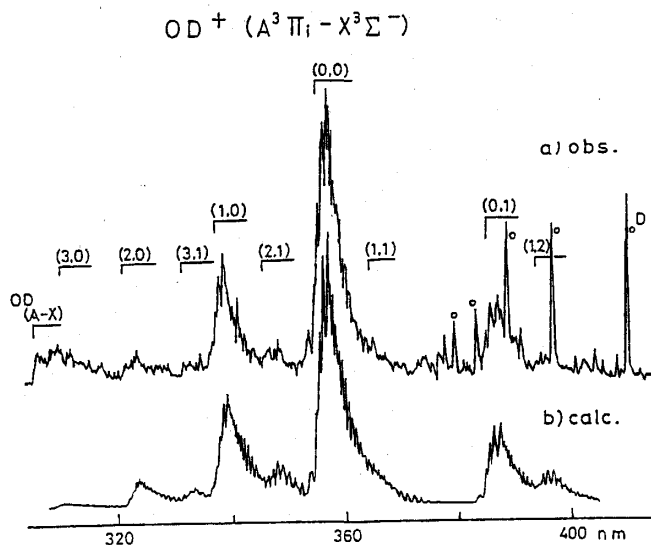
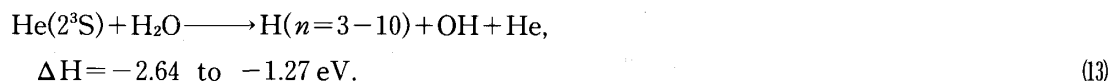


Fig. 5 Emission spectra of D_2O .
(a) Beam: obs. (b) Beam: Calc.

most prominent band in both spectra is the $\text{OH}^+(A^3\Pi - X^3\Sigma^-)$ system from $v' = 0-3$. In addition, emissions from neutral fragments, $\text{OH}(A^2\Sigma^+ - X^2\Pi)$ and H (Balmer series), are identified. In the beam experiment, the $\text{OH}^+(A-X)$ and $\text{OH}(A-X)$ bands disappeared almost completely by the ion trapping, while the H^* lines were independent of the ion trapping. From these facts and the ener-

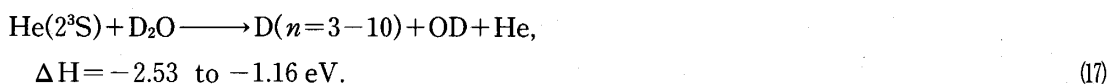
getics, the excited fragments are found to be formed through the following processes:



An outstanding feature of the FA spectrum is that the OH(A-X) band is enhanced in comparison with the beam spectrum. This is a consequence of fast electron-ion recombination process (14) in the high pressure FA experiment.^{36, 37)}



The reactions of He active species with D₂O in the beam experiment gave the corresponding isotopic band systems as shown in Fig. 5a). Based upon the energetics and the effect of ion trapping, OD⁺(A-X), OD(A-X), and deuterium Balmer lines are found to be excited through the following processes:



This report focuses upon dissociative ionization (11) and (15). The rovibrational distributions of OH⁺(OD⁺) in the A³Π state were determined by a computer simulation of the observed spectra. Twenty seven rotational branches were involved in the calculation and the dependence of FA factors on the rotational quantum number was taken into consideration. The best fit spectra are shown in Fig. 4b) for OH⁺(A-X) and Fig. 5b) for OD⁺(A-X). The rovibrational distributions obtained in the beam and FA experiments are summarized in Table 5 along with the ICR data of Govers *et*

Table 5 Rovibrational distributions of OH⁺(OD⁺) in the A³Π_i state.

		<i>v'</i> = 0	1	2	3
OH ⁺	Obs. (This work)	0.66	0.20	0.10	0.04
	Obs. (ICR) ^{a)}	0.63	0.25	0.12	—
	Calc. (2-body) ^{b)}	0.30	0.26	0.23	0.21
	T _r	1700 ± 200 K			
OD ⁺	Obs. (This work)	0.55	0.26	0.13	0.06
	Obs. (ICR) ^{a)}	0.63	0.25	0.12	—
	Calc. (2-body) ^{b)}	0.28	0.26	0.24	0.22
	T _r	1800 ± 200 K			

a) Ion cyclotron resonance data in Ref. 38.

b) Statistic prior distributions calculated assuming two-body dissociation model.

ing two-body dissociation model for the formation of the OH⁺(A) and OD⁺(A) fragments:



The prior vibrational distributions obtained from the relation $(1-f_v)^{3/2}$ are more excited than the experimental ones. A similar disagreement was found for the rotational distributions between the prior distributions and the experimental ones. For example, rotational energy of OH⁺(A : $v'=0$) is predicted to be 1.23 eV from the relation $g_r = f_r / (1-f_v)$. This value is much larger than the observed ones (0.15 eV). Large discrepancies between the statistical and experimental rovibrational distributions suggest that the internal energy distributions of OH⁺(A) and OD⁺(A) produced from the dissociation of precursor H₂O⁺⁺(D₂O⁺⁺) ions are not controlled by the statistical factor.

The authors thank Drs. Hiroshi Obase, Sumio Yamaguchi, and Minoru Endoh for their co-operation. This work was supported by a Grant-in-Aid for Scientific Research (No. 61540353, 63540373, 02640371, and 02555170) from the Ministry of Education, Science, and Culture, the Asahi Glass Foundation, and the Ito Science Foundation.

References

- 1) E.E. Ferguson, F.C. Fehsenfeld, and A.L. Schmeltekopf, *Adv. At. Mol. Phys.*, **5**, 1 (1969).
- 2) D.L. Albritton, *At. Data Nucl. Data Tables*, **22**, 1 (1978).
- 3) M. Tsuji, in *Techniques of Chemistry: Techniques for the Study of Ion Molecule Reactions*, Eds. by J.M. Farrar and W. Saunders Jr., (John Wiley & Sons, New York, 1988), pp 489-562.
- 4) M. Tsuji, I. Murakami, and Y. Nishimura, *J. Chem. Phys.*, **75**, 5373 (1981).
- 5) S. Yamaguchi, M. Tsuji, and Y. Nishimura, *Chem. Phys. Lett.*, **138**, 29 (1987).
- 6) M. Tsuji, T. Mizuguchi, and Y. Nishimura, *Can. J. Phys.*, **59**, 985 (1981).
- 7) Y. Nishimura, *Rep. Res. Inst. Ind. Sci., Kyushu University*, **80**, 111 (1986).
- 8) M. Tsuji, T. Mizuguchi, and Y. Nishimura, *Chem. Phys. Lett.*, **84**, 318 (1981).
- 9) M. Tsuji, K. Shinohara, S. Nishitani, T. Mizuguchi, and Y. Nishimura, *Can. J. Phys.*, **62**, 353 (1984).
- 10) M. Tsuji, AIP Conference Proceedings 205, *The Physics of Electronic and Atomic Collisions, XVI Int. Conf. New York, NY 1989*, Edited by A. Dalgarno, R.S. Freund, P.M. Koch, M.S. Lubell, and T.B. Lucartorto, AIP, NY, (1990), pp. 342-349.
- 11) J.C. Creasey, I.R. Lambert, R.P. Tuckett, and A. Hopkirk, *J. Chem. Soc. Faraday Trans.*, **86**, 2021 (1990).
- 12) M. Tsuji, J.P. Maier, H. Obase, and Y. Nishimura, *Chem. Phys.*, **110**, 17 (1986).
- 13) H. Obase, M. Tsuji, and Y. Nishimura, *Chem. Phys.*, **57**, 89 (1981).
- 14) H. Obase, M. Tsuji, and Y. Nishimura, *Chem. Phys.*, **74**, 89 (1983).
- 15) M. Tsuji, J.P. Maier, H. Obase, H. Sekiya, and Y. Nishimura, *Chem. Phys. Lett.*, **137**, 421 (1987).
- 16) M. Tsuji, K. Tsuji, H. Fukutome, and Y. Nishimura, *Chem. Lett.*, **673** (1977).
- 17) H. Obase, M. Tsuji, and Y. Nishimura, *Chem. Phys. Lett.*, **141**, 133 (1987).
- 18) M. Tsuji, K. Mizukami, H. Obase, and Y. Nishimura, *J. Phys. Chem.*, **92**, 1163 (1988).
- 19) M. Endoh, M. Tsuji, and Y. Nishimura, *Chem. Phys.*, **82**, 67 (1983).
- 20) M. Tsuji, H. Obase, M. Endoh, S. Yamaguchi, K. Yamaguchi, K. Koburai, and Y. Nishimura, *J. Chem. Phys.*, **89**, 6753 (1988).
- 21) H. Sekiya, M. Tsuji, and Y. Nishimura, *Chem. Lett.*, 1997 (1986).
- 22) H. Obase, M. Tsuji, and Y. Nishimura, *J. Chem. Phys.*, **87**, 2695 (1987).

Optical Spectroscopic Studies on Ionization Processes by Using Flowing Afterglow

- 23) M. Tsuji and J.P. Maier, *Chem. Phys.*, **126**, 435 (1988).
- 24) H. Sekiya, M. Tsuji, and Y. Nishimura, *J. Chem. Phys.*, **87**, 325 (1987).
- 25) S. Yamaguchi, M. Tsuji, and Y. Nishimura, *J. Chem. Phys.*, **88**, 3111 (1988).
- 26) S. Yamaguchi, M. Tsuji, and Y. Nishimura, *J. Chem. Phys.*, **87**, 1637 (1987).
- 27) S. Yamaguchi, M. Tsuji, H. Obase, H. Sekiya, and Y. Nishimura, *J. Chem. Phys.*, **86**, 4952 (1987).
- 28) W.W. Robertson, *J. Chem. Phys.*, **44**, 2456 (1966).
- 29) W.C. Richardson, D.W. Setser, D.L. Albritton, and A.L. Schmeltekopf, *Chem. Phys. Lett.*, **12**, 349 (1971).
- 30) W.C. Richardson and D.W. Setser, *J. Chem. Phys.*, **58**, 1809 (1973).
- 31) D.S.C. Yee, W.B. Stewart, C.A. McDowell, and C.E. Brion, *J. Electron Spectrosc.*, **7**, 93 (1975).
- 32) H. Hotop and G. Hübler, *J. Electron Spectrosc.*, **11**, 101 (1977).
- 33) H. Hotop, E. Kolb, and J. Lorenzen, *J. Electron Spectrosc.*, **16**, 213 (1979).
- 34) O. Leisin, H. Morgner, and W. Müller, *Z. Phys.*, **A304**, 23 (1982).
- 35) K. Mitsuke, T. Takami, and K. Ohno, *J. Chem. Phys.*, **91**, 1618 (1990).
- 36) C. B. Collins and W.W. Robertson, *J. Chem. Phys.*, **40**, 701 (1964).
- 37) A.J. Yencha and K.T. Wu, *Chem. Phys.*, **32**, 247 (1978).
- 38) T.R. Govers, M. Gérard, and R. Marx, *Chem. Phys.*, **15**, 185 (1976).
- 39) J. Appell and J. Durup, *Int. J. Mass Spectrom. Ion Phys.*, **10**, 247 (1972/73).